Spectrochimica Acta Part A: Molecular and Biomolecular Spectroscopy 291 (2023) 122374

Contents lists available at ScienceDirect

Spectrochimica Acta Part A:
Molecular and Biomolecular Spectroscopy

journal homepage: www.journals.elsevier.com/spectrochimica-acta-part-a-molecular-and-biomolecular-spectroscopy

Validation of spectrophotometric method to quantify chloramphenicol in fluid and rat skin tissue mimicking infection environment: Application to *in vitro* release and *ex vivo* dermatokinetic studies from dissolving microneedle loaded microparticle sensitive bacteria

Mukarram Mudjahid , Sulistiawati , Rangga Meidianto Asri , Firzan Nainu , Andi Dian Permana *

Faculty of Pharmacy, Hasanuddin University, Makassar 90245, Indonesia

HIGHLIGHTS

- A spectrophotometric method to quantify chloramphenicol (CHL) was developed.
- The analytical method was validated according to ICH guidelines.
- Formulation of dissolving microneedle (DMN) loaded microparticles CHL was developed.
- Validated method was applied in *in vitro* release study of microparticles CHL.
- The validated method was applied in *ex vivo* dermatokinetic study of DMN.

GRAPHICAL ABSTRACT

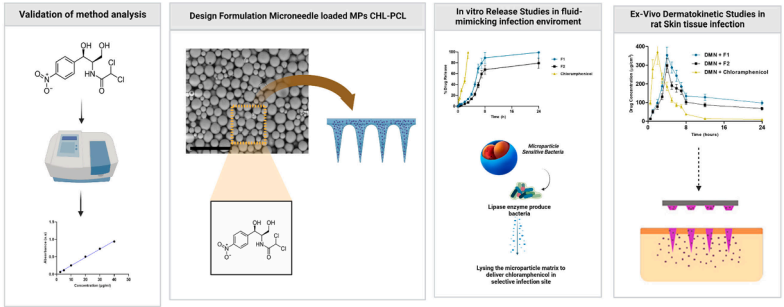

ARTICLE INFO

Keywords:
Bacterially sensitive microparticles
Cellulitis
Chloramphenicol
Microneedle
UV–vis spectrophotometry
Validation

ABSTRACT

Cellulitis is a common dermis/subcutaneous tissue skin infection and shared global disease burden, with a higher incidence for males and people aged 45–64 years. Application therapy of chloramphenicol (CHL) has been hindered because of its toxicity and limited penetration into the skin. In this research, CHL was developed into a bacterially sensitive microparticles which were further incorporated into a microneedle system to increase penetration. To support this formulation, in this study, UV–vis spectrophotometry method was validated in methanol, polyvinyl alcohol (PVA) 1%, phosphate buffered saline (PBS), tryptic soy broth (TSB) (fluid-mimicking infection), and skin tissue to quantify amount of CHL. The developed analytical method was subsequently validated according to ICH guidelines. The results obtained showed that the correlation coefficients were linear ≥0.9934. The values of LLOQ inside the methanol, PVA 1%, PBS, TSB, and skin tissue were 7.20 μg/mL, 4.40 μg/mL, 8.18 μg/mL, 387.48 μg/mL, and 7.27 μg/mL, respectively. The accuracy and precision of the developed method were prominent. These methods were successfully applied to quantify the amount of CHL in microparticle and microneedle system in fluid and tissue skin infection. The result showed the high drug release microparticle sensitive bacteria, and high drug retention in *ex vivo* dermatokinetic evaluation in rat skin tissue containing bacterial infection. This was due to the presence of *Staphylococcus aureus* bacteria culture that

* Corresponding author.
E-mail address: andi.dian.permana@farmasi.unhas.ac.id (A. Dian Permana).

https://doi.org/10.1016/j.saa.2023.122374
Received 3 August 2022; Received in revised form 15 December 2022; Accepted 12 January 2023
Available online 18 January 2023
1386-1425/© 2023 Elsevier B.V. All rights reserved.

produced lipase enzymes, playing a role in lysing microparticle matrix to develop selectively delivery antimicrobials. A further analytical method needs to be matured to quantify CHL inside the *in vivo* studies.

1. Introduction

Cellulitis is a type of soft infection in the dermis / subcutaneous tissue characterized by warmth, erythema, and pain due to the response of cytokines and neutrophils from bacteria that penetrate the epidermis [1,2]. Cellulitis is a shared global disease burden. Its incidence rate is 24.6/1000 person-years, and it is more common in men and people between the ages of 45 and 64. [3]. The location of the infection in the cutaneous tissue with no visible wound in the epidermis of the skin has been often ignored as ordinary inflammation. These symptoms are also typical in other inflammatory skin conditions, making identification of wound-related cellulitis difficult, while bacterial culture is quickly developing. [4]. It is possible to enhance the degree of chronic wounds that were difficult to heal and required treatment management extension.

The microorganisms most commonly associated with cellulitis infection are *Staphylococci* and -hemolytic *streptococci* bacteria group [5,6]. Multibacterial colonization with different strains of human skin tissue has been widely reported [7]. This is associated with the interaction of bacteria with different strains that can synergize the severity of the disease [8]. Accordingly, broad-spectrum antibiotics are considered in the selection of therapy.Chloramphenicol (CHL) as broad antibiotic is active against gram- positive, gram-negative bacteria and anaerobic microorganisms [9,10]. Oral administration of CHL produces systemic effects and has been associated with significant side effects, hematological disorders (aplastic anemia), spinal cord suppression, and availability of inadequate drug concentrations in specific infectious tissues [11]. Therefore, it requires a long time for treatment. To overcome these shortcomings, CHL could be designed in dermal preparations to reduce systemic exposure and increase drug concentrations to adequate target tissues of interest.

During the last decade, dermal delivery systems have been developed by designing drugs into microparticles/nanoparticles [12]. Microparticles are preferred to local infection targets with a longer drug retention rate in skin tissue than nanoparticles [13,14]. The system can be designed to adapt release of the drug to the specific infected area [15,16]. The tissue's properties result in lower pH, greater temperature, surface proteins, and increased production of bacterial toxins, which function as a trigger for infection responsive delivery. [17].

Enzymes are considered promising since, under mild conditions, the enzymatic reactions are more efficient and accurate. Moreover, they are also necessary for the bacterial metabolic and pathological processes [18]. The chemical synthesis of bacterial lipase-sensitive PCL for specific delivery of antimicrobials was recently reported [19]. It has been reported, that SA may release a particular enzyme called lipolytic esterase (Lipase), this enzyme can initiate the biocatalytic hydrolysis of PCL [19]. Thus, lipase production at infection sites may be utilized to deliver and prove a practical, safe treatment approach selectively. This principle led to the development of delivery systems that selectively deliver drugs to specific sites of infection and reduce toxicity which is minimal when administered dermally.

Due to its hydrophobic chemical composition, which prevents effective cutaneous penetration, CHL is not useful for topical treatment of skin infections. Additionally, because human skin is thicker, it creates an impenetrable barrier that prevents the transdermal delivery of hydrophobic drugs. Dissolving microneedles (DMN) have the ability to penetrate biofilms and necrotic tissue in diseased skin by-passing the primary skin barrier [20] and may dissolve larger needles that are embedded in the skin. Importantly, the administration of DMN has the benefits of localized, painless, quick delivery, and patient compliance [21]. Given the potential advantages of this strategy, adding microparticles (MPs) chloramphenicol to DMNs may enhance the quantity of CHL that penetrate biofilm and necrotic tissue on diseased skin, which may help the treatment of burns and chronic wounds.

A fundamental part of developing new drug delivery systems is detecting and quantifying the drug, and therefore, it is crucial to develop an appropriate analytical method. In this research, the determination of drug content and the amount of drug release concentration from the *in vitro* method are critical assessments while developing a bacterial-responsive microparticle system. *In vitro* studies are the first phase of evaluating drug release profiles using relevant release media.

In measuring CHL in various matrices, numerous systematic methods have been developed until now. This includes both reseacrh articles HPLC-UV [22] and HPLC-MS/MS [23]. However, the reported method are unsuitable for a limited budget and time. It also requires sophisticated equipment, making it a challenge to implement this in countries/laboratories with middle to low-income [24]. In contrast, the promise of UV–vis spectrophotometers utilized in detecting and quantifying CHL is due to their simplicity and cost-effectiveness. This study developed a CHL quantification method in artificial infection media and artificial skin fluids. There have been reports from some previous studies that the ability of UV–vis spectrophotometers to quantify various types of drugs [24–26]. It was crucial to validate the method used to ensure that the development of analytical procedures is reliable, comparable, and traceable.

This study aimed to develop and validate a method for analyzing CHL in fluid and rat skin tissue mimicking infection environment where the UV–vis spectrophotometer was utilized. The next step was to validate the method in accordance with the guidelines of international conference harmonization (ICH). The evaluated parameters were linearity, accuracy, precision, the limit of detection (LOD), and the limit of quantification (LOQ). Finally, the validated approach was used to determine the drug concentration CHL in the MPs system, the drug release profile *in vitro*, and *ex vivo* dermatokinetic investigations from DMN loaded MPs sensitive bacteria.

2. Materials and methods

2.1. Material

Chloramphenicol (CHL) was purchased from Merck (Darmstadt, Germany). Polycaprolactone (PCL), polyvinyl alcohol (PVA), polyvinyl pyrrolidone (PVP), sodium chloride, tryptic soy broth (TSB), potassium chloride, disodium phosphate, and potassium dihydrogen phosphate, were obtained from Sigma-Aldrich (Singapore). All other reagents used were analytical grade.

2.2. Preparation of CHL stock solution

The stock solution of CHL was prepared in 2 concentrations, where 10 mg and 20 mg CHL were weighed into a 10 mL volumetric flask. After that, to dissolve the CHL, methanol was added to the solutions with concentrations of 1000 μg/mL and 2000 μg/mL were obtained, respectively.

2.3. Measurement of the maximum UV absorption wavelength, testing standard, and quality control specimen preparation.

UV–vis spectrophotometer (Dynamica, HELLO XB-10) was employed to determine the maximum wavelength absorbance. The CHL solution was prepared in concentration of 10 μg/mL in methanol, PVA 1%, PBS media, and 750 μg/mL in TSB media. The solution was scanned at room

Table 1
Quantity of organic solvent required to extract CHL from skin tissue samples.

Organic Solvent	Methods	Volume (mL)
Methanol	A	1
	B	3
	C	5
	D	7
Acetonitrile	A	1
	B	3
	C	5
	D	7

Table 2
Composition of formulations MPs loaded with CHL.

Composition	F1	F2
PCL (mg/7 mL chloroform)	35	70
CHL (mg/3 mL methanol)	35	35
PVA 3% (mL)	25	25

temperature at a 200–400 nm wavelength. Subsequently, six concentrations ranging from 2.5 μg/mL to 40 μg/mL on methanol, PBS, PVA 1%, skin tissue and 125 μg/mL–1250 μg/mL on TSB media were prepared as calibration solutions.

Moreover, in an attempt to ensure the samples meet the expected criteria, each solvent was used as quality control (QC) samples at four quality levels, which are lower limit of quantification (LLOQ), low quality control (LQC), medium quality control (MQC), and high quality control (HQC). All parameters were measured and prepared in 3 replications.

2.4. Sample preparation and CHL extraction from skin samples

To prevent any interferences with the measurement, the skin tissue sample was prepared by precipitating the proteins and other molecules present in the organ. Methanol and acetonitrile were used to carry out the CHL extraction procedure. As stated in Table 1, different amounts of acetonitrile and methanol were employed to extract the drug. In the beginning, 1 g of the CHL spiked with matrices was combined with the extraction solvent. The mixture was then centrifuged at 14000 rpm for 15 min after being homogenized for 10 min using a vortex mixer. The obtained supernatant was then left at room temperature to allow the organic solvent to evaporate. The dried extract was then reconstituted with 1 mL of methanol, homogenized, and centrifuged as before. The resulting supernatant was then evaluated using UV–vis spectrophotometry.

2.5. Preparation of chloramphenicol sensitive bacterial microparticles (MPs CHL-PCL) and microneedle loaded MPs CHL-PCL

MPs CHL-PCL were prepared by a solvent evaporation method using polycaprolactone (PCL) as polymer and polyvinyl alcohol (PVA) as surfactant. Chloroform and methanol were used as solvents for the organic phase. Briefly, PCL was dissolved in 7 mL of chloroform, and CHL was dissolved in 3 mL of methanol, then mixed until homogeneous. The aqueous phase was prepared using PVA 3% solution (see Table 2). The organic phase was added to the aqueous phase and mixed using a mechanical homogenizer at 500 rpm for 5 min. The emulsion system obtained was kept for 5 h under a magnetic stirrer to ensure the organic phase evaporated completely. The formed MPs were then collected by centrifugation and washed with distilled water three times, separated and stored in a desiccator until dry.

The dissolving microneedle (DMN) preparations were created. In this investigation, a silicone mold and the centrifugation process were applied. The mold used possessed several parameters, including a density of 10x10, pyramidal needles with a height of 700 μm, a base width of 200 μm, and an interspacing of 200 μm. Each formulation (F1 and F2) contained 1 g of the formula, which contains MPs CHL-PCL 30%, PVP K-30 25%, PVA 10%, and Aquadest 35%. MPs CHL-PCL was combined with the polymer mixture to create the DMN that hold the active ingredient. They were then subjected to sonication until a clean, bubble-free dispersion was achieved. The polymer-drug combination was then put on the mold and centrifuged (LC-04S Centrifuge, Zenith Lab (Jiangsu) Co., LTD.) for 30 min at 3500 rpm. When the centrifugation process was completed, the excess polymer mixture at the top of the mold was removed and replaced with a fresh polymer mixture. The MN were then dried for 1 day at room temperature and 1 day at 37 °C without being removed from the mold [27].

2.6. Validation of analytical methods

2.6.1. Specificity

The comparison of the UV wavelength spectrum of CHL standard solutions in various solvent media is used as an indicator for the specificity parameter. The assessed parameter was used to identify the possibility of interference among the analyte and the response of an alternative synthesis at the appropriate wavelength.

2.6.2. Linearity calibration curve

Parameters of the linear measurement of each medium were assessed with six standard solutions focusing on the appropriate wavelength spectrum. The results were projected in a calibration curve consisting of six concentrations with the obtained absorbance results. Parameters of determination coefficient (r^2), slope, and y-intercept were then obtained and analyzed [28].

2.6.3. Limit of detection (LOD)

The parameter represents the minimum analyte concentration that can be measured with a sample [29]. LOD was determined using the equation. (1) below, that the blank ideal divergence (without specimen) was symbolled by “sy”, and the slope applied through the calibration curve regression equation was symbolled by “b”.

$$\mathrm{LOD} = \frac{3.3\mathrm{sy}}{\mathrm{b}} \quad (1)$$

2.6.4. Lower limit of quantification (LLOQ)

A minimum sample absorption that can be precisely calculated with satisfying precision and accuracy is called the parameter of LLOQ [28]. LLOQ is determined using the equation. (2) below, that the blank ideal divergence (without specimen) was symbolled by “sy”, and the slope applied through the calibration curve regression equation was symbolled by “b”. [30].

$$\mathrm{LLOQ} = \frac{10\mathrm{sy}}{\mathrm{b}} \quad (2)$$

2.6.5. Accuracy and precision

The precision and the accuracy of parameters specify the propinquity to the reference value and the degree of a series of measurements applied from several tests in the scientific method. These variables were assessed by measuring the inter-day and intra-day QC samples, which are HQC, QMC, LQC, and LLOQ. Percent relative error (%RE) and relative standard deviation (%RSD) were determined to express a quality that is accurate along with precise [31].

2.6.6. Extraction recovery

The absolute extraction recovery determination was calculated by comparing the response value of CHL in quality control samples (LLOQ, LQC, MQC, and HQC) from skin tissue to those obtained for freshly prepared solutions of the concentrations of the same samples (LLOQ, LQC, MQC, and HQC) [29].

Table 3
Mean extraction recovery of CHL of each method with methanol and acetonitrile from skin tissue (n = 3).

Organic Solvent	Methods	Volume (mL)	%Extraction Recovery ± SD	% RSD
Methanol	A	1	18.52 ± 1.90	10.26
	B	3	41.78 ± 1,24	2.97
	C	5	91.54 ± 2.67	2.91
	D	7	94.77 ± 0.96	1.01
Acetonitrile	A	1	12.18 ± 0.82	6.72
	B	3	12.45 ± 3.11	24.96
	C	5	39.92 ± 1.90	4.74
	D	7	62.38 ± 3.27	5.24

2.7. Application of analytical methods

2.7.1. Size estimation calculation and particle size distribution

Particle size was calculated using a microscopic method using an optical microscope equipped with a digital camera for as many as 300 particles. To see the shape and surface of the CHL MPs produced. Analysis of the particle size distribution by looking at the polydispersity index (PDI) value using the equation.

$$PDI = \left(\frac{Standard\ \ deviation}{mean\ \ particles\ \ diameter}\right)^2 \quad (3)$$

2.7.2. Calculation of % encapsulation and drug loading efficiency

The MPs suspension was centrifuged, the supernatant was taken, and then analyzed using a UV–vis spectrophotometer at a maximum wavelength of 274.8 nm. The calculation of % encapsulation efficiency (EE) and % drug loading (DL) follows the following equation:

$$\%DL = \frac{Amount\ \ of\ \ Encapsulated\ \ Drug}{Total\ \ Weight} 100 \quad (4)$$

$$\%EE = \frac{Drug\ \ Total - Drug\ \ Free}{Drug\ \ Total} x100 \quad (5)$$

2.7.3. Drug content measurement of DMN loaded CHL-PCL

The needles in the DMN are taken out by scraping the needle, then the needles are dissolved in water. After that, the solution was then centrifuged at 5000 rpm for 10 min. The precipitated MPs were then dissolved with an organic solvent (methanol: chloroform) to remove the polymer matrix. The samples were then analyzed using a UV–vis spectrophotometer to measure drug content.

2.7.4. In vitro release study of microparticle sensitive bacteria in bacterial culture

The *In vitro* release study of MPs was conducted to evaluate the sensitivity of bacteria to polymers by designing MPs on media containing the presence or absence of bacteria. In bacterial culture media, MPs dispersed in 20 mL of bacterial culture (equivalent to 0.5 Mc Farland) were placed in an orbital stirrer at 100 rpm, temperature 37 ± 1 °C. Samples (500 μL volume) were then taken at predetermined time points (0,5, 2, 4, 6, 8, 12, and 24 h). The sample was then centrifuged at 10,000 rpm for 15 min, and the concentration was calculated with a UV–vis spectrophotometer.

2.7.5. Ex vivo dermatokinetic studies on infection skin rat model of microneedle preparation

2.7.5.1. Preparation of ex vivo model of infection on rat skin. Prior to the

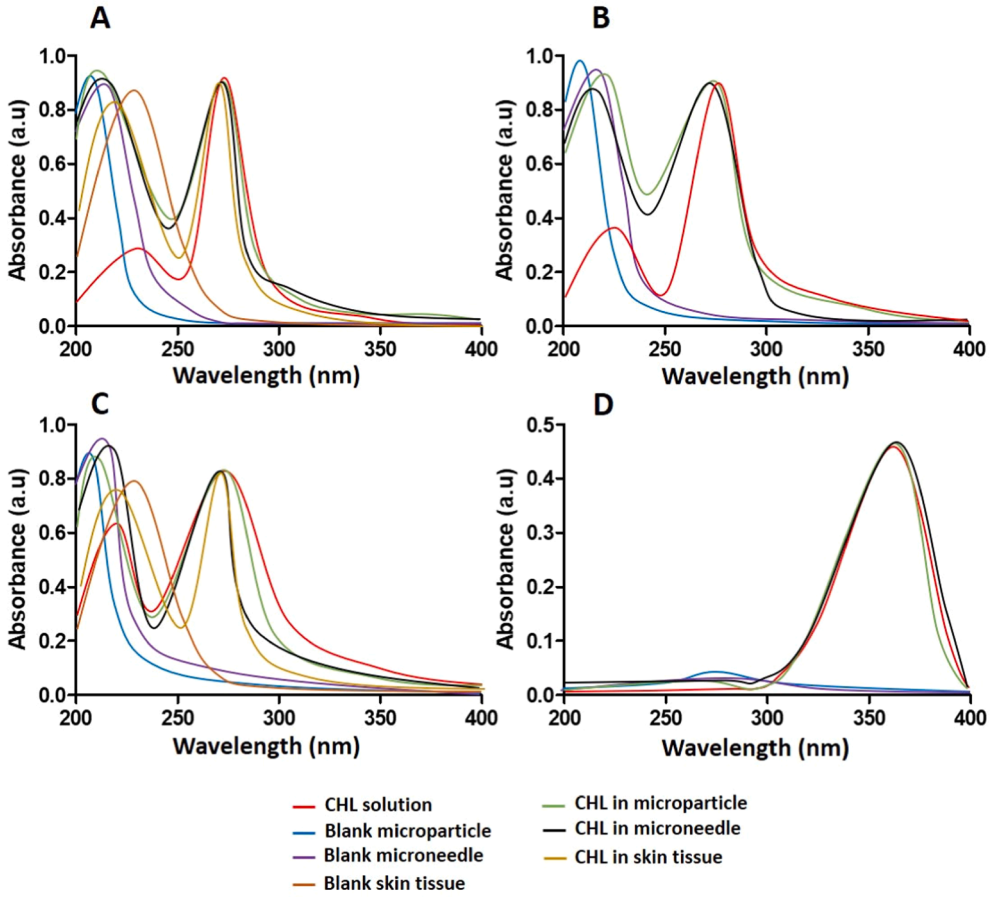

Fig. 1. Representative UV spectra of CHL and several blank in Methanol (A), PVA (B), PBS (C), TSB (D).

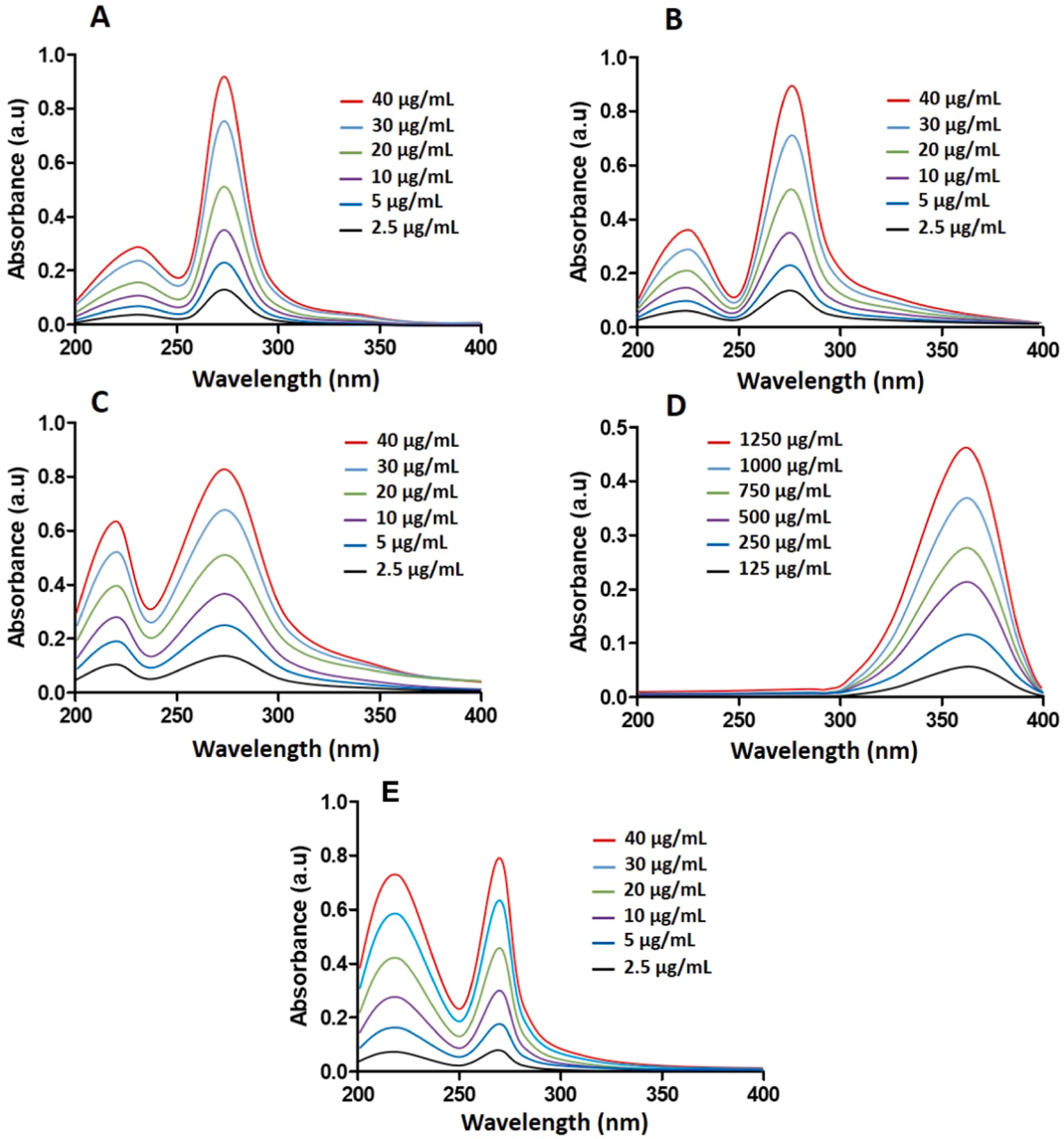

Fig. 2. Spectrum of CHL standard solutions in of Methanol (A), PVA (B), PBS (C), TSB (D), Skin Tissue (E).

Table 4
Calibration curve properties for CHL analysis with the quality of LOD and LLOQ.

Media	Concentration Range (µg/mL)	r^2	LOD. (µg/mL)	LLOQ. (µg/mL)
MeOH	2.5–40	0.9981	2.37	7.20
PVA 1%	2.5–40	0.9993	1.45	4.40
PBS	2.5–40	0.9975	2.70	8.18
TSB	125–1250	0.9934	127.87	387.48
Skin Tissue	2.5–40	0,9981	2.40	7.27

experiment, Wistar rat abdominal skins were shaved and adjusted in PBS (pH 7.4). The rat skins were cleaned in ethanol at a 70 percent concentration for one hour. The ethanol in the skins was evaporated before use by placing them in a biosafety cabinet for 20 min. Briefly, a biopsy punch was used to make a wound in the skin's surface (Stiefel, Middlesex, UK). Then, with a few minor adjustments, the earlier published protocols were used to create *ex vivo* models of biofilm on rat skin [32]. After that, 50 µL of the diluted SA bacterial suspensions (2×10^5 CFU/mL) were dripped to the wound of the skin and distributed evenly after the skins were mounted on TSA plates. The skins were transferred to fresh TSA plates every day for five days while the plates were incubated at 37 °C to facilitate the growth of the biofilm on the injured skin.

2.7.5.2. Ex vivo dermatokinetic studies. The ex vivo dermatokinetic studies were also evaluated Using the procedure outlined [20,32] with slight modification. Ex vivo dermatokinetic experiments of DMN containing MPs CHL-PCL were conducted in normal skin and ex vivo infection model in rat skins. The skins that had previously been fastened to the donor compartment of the Franz diffusion cells were manually placed for 30 s. The receiver compartment, which contained PBS, was further connected to the donor compartment (pH 7.4). Afterwards, 5 g of stainless-steel mass was used on top of the DMN to prevent movement during the trial. The experiment was conducted at 600 rpm and 37 ± 1 °C. The DMN were separated from the skins in order to assess the concentration of CHL in the skins at various specified time intervals. The skins were cleaned three times, put into glass vials, and given 2.5 mL of water. The mixtures were centrifuged at 3000 rpm for 15 min after being vortexed for 30 min. UV–vis spectrophotometer was used to measure the CHL content in the supernatant. PKSolver (China Pharmaceutical University, Nanjing, China) was used to construct the dermatokinetic profiles [34].

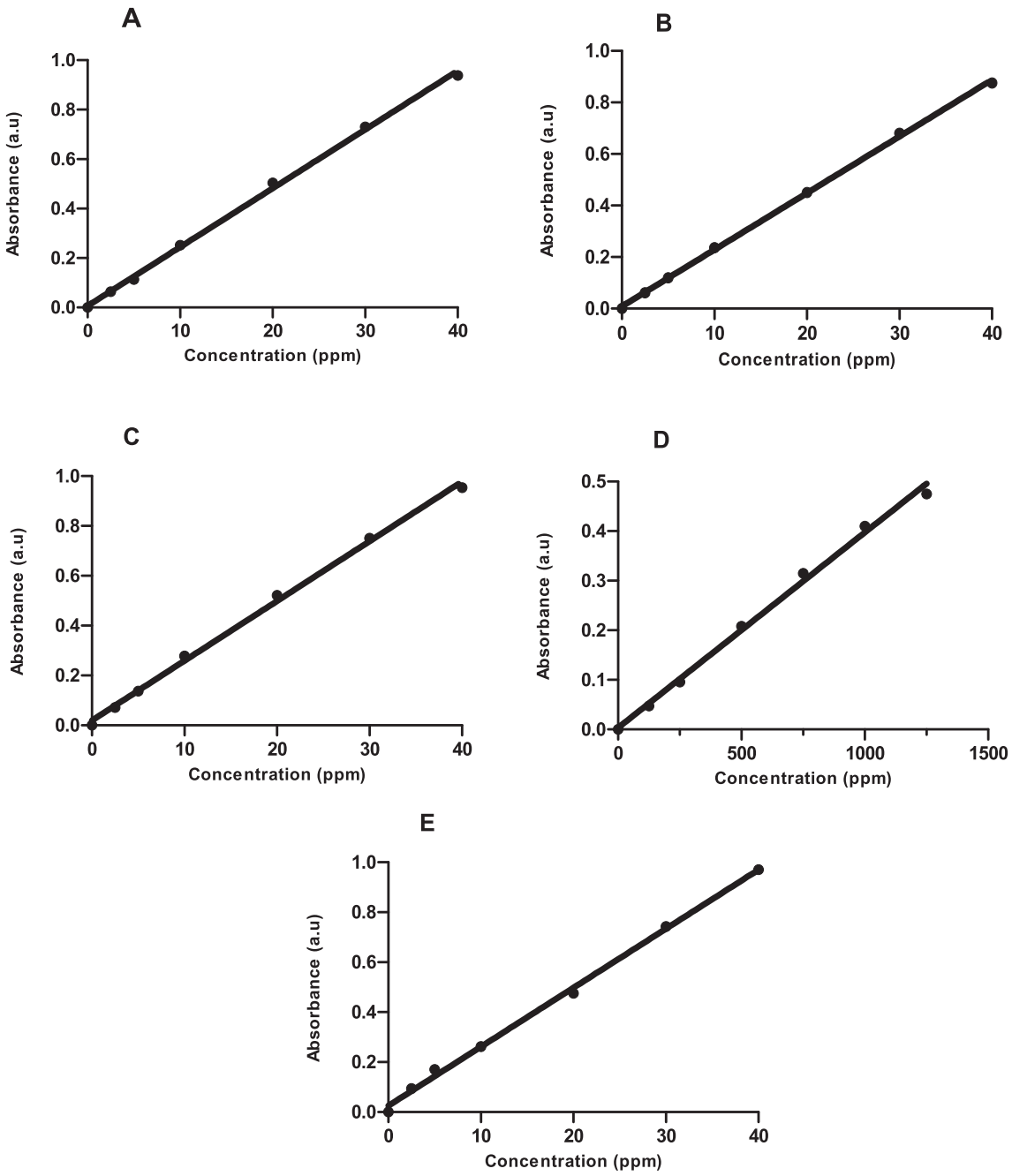

Fig. 3. Calibration Curves CHL-Methanol (A), CHL-PVA (B), CHL-PBS (C), CHL –TSB (D), CHL-Skin Tissue (E).

2.8. Statistical analysis

All results were reported as means ± standard deviation (SD). The mean, SD, linear regression analysis, %RSD and %CV of each sample in the validation method were processed using Microsoft® Excel 2016 (Microsoft Corporation, Redmond, Washington, USA). GraphPad Prism® version 6 (GraphPad Software, San Diego, California, USA) was utilised to statistically analyse the results where a p-value < 0.05 denoted a significant difference.

3. Results and discussion

3.1. Selection of sample preparation method and drug extraction

In this study, methanol and acetonitrile, two organic solvents, were used to extract CHL from skin tissue. Table 3. displays the outcomes of every extraction technique. The findings demonstrated that the extraction efficiency might be increased by using more solvent during the extraction procedure. Methanol offered a greater extraction recovery than acetonitrile, it was also discovered. The findings indicated that techniques C and D had the greatest extraction recovery percentages for extracting CHL from methanol, with respective values of 91.54 ± 2.67 percent and 94.77 ± 0.96 percent. Furthermore, both of these approaches were not a significantly difference ($p > 0.05$). Because it required the least quantity of solvent while still providing the best extraction recovery, method C (5 mL methanol) was selected as the best extraction technique for this investigation.

Table 5
The Results of evaluation of precision and accuracy of CHL analysis in PVA 1% (mean ± SD, n = 3).

Interday Precision and Accuracy				
Replication	**Concentration added (μg/mL)**	**Found concentration (μg/mL) ± SD**	**Precision (%RSD)**	**Accuracy (%RE)**
1	4.40	4.29 ± 0.070	1.63	2.53
	7.5	7.36 ± 0.05	0.72	1.75
	30	30.28 ± 0.12	0.39	0.96
	15	14.52 ± 0.069	0.48	3.17
2	4.40	4.16 ± 0.11	2.66	5.37
	7.5	7.44 ± 0.07	1.01	0.76
	30	30.09 ± 0.14	0.48	0.3
	15	14.43 ± 0.07	0.48	3.78
3	4.40	4.43 ± 0.09	2.16	−0.59
	7.5	7.67 ± 0.04	0.59	−2.32
	30	30.77 ± 0.07	0.23	2.59
	15	14.79 ± 0.16	1.08	1.34
Intraday Precision and Accuracy				
Day	**Concentration added (μg/mL)**	**Found concentration (μg/mL) ± SD**	**Precision (%RSD)**	**Accuracy (%RE)**
1	4.40	3.77 ± 0.046	1.21	14.32
	7.5	6.89 ± 0.05	0.72	8.11
	30	30.08 ± 0.09	0.31	0.29
	15	13.49 ± 0.09	0.67	10
2	4.40	3.85 ± 0.02	0.67	12.59
	7.5	7.32 ± 0.09	1.30	2.36
	30	29.92 ± 0.09	0.30	−0.26
	15	13.43 ± 0.14	1.06	10.42
3	4.40	3.91 ± 0.04	1.17	11.21
	7.5	7.36 ± 0.14	1.90	1.76
	30	30.28 ± 0.09	0.30	0.96
	15	13.74 ± 0.07	0.51	8.37

Table 6
The Results of evaluation of precision and accuracy of CHL analysis in MeOH (mean ± SD, n = 3).

Interday Precision and Accuracy				
Replication	**Concentration gained (μg/mL)**	**Found concentration (μg/mL) ± SD**	**Precision (%RSD)**	**Accuracy (%RE)**
1	7.2	7.30 ± 0.11	1.51	−1.48
	10	10.73 ± 0.08	0.79	−7.36
	30	32.55 ± 0.11	0.34	8.51
	20	22.18 ± 0.08	0.39	−10.93
2	7.2	7.35 ± 0.10	1.43	−2.08
	10	10.86 ± 0.08	0.78	−8.63
	30	32.76 ± 0.11	0.34	9.21
	20	22.27 ± 0.09	0.41	−11.36
3	7.2	7.40 ± 0.14	2.02	−2.87
	10	10.79 ± 0.13	1.22	−7.93
	30	32.27 ± 0.23	0.71	7.57
	20	22.23 ± 0.12	0.57	−11.15
Intraday Precision and Accuracy				
Day	**Concentration gained (μg/mL)**	**Found concentration (μg/mL) ± SD**	**Precision (%RSD)**	**Accuracy (%RE)**
1	7.2	7.87 ± 0.13	1.65	−9.30
	10	10.61 ± 0.15	1.45	−6.1
	30	31.14 ± 0.10	0.32	3.82
	20	21.41 ± 0.14	0.69	−7.06
2	7.2	8.03 ± 0.12	1.55	−11.62
	10	10.75 ± 0.10	0.98	−7.5
	30	31.28 ± 0.30	0.97	4.27
	20	21.66 ± 0.26	1.22	−8.31
3	7.2	8.16 ± 0.04	0.55	−13.37
	10	10.86 ± 0.12	1.15	−8.66
	30	31.2 ± 0.17	0.54	4
	20	21.48 ± 0.10	0.49	−7.41

3.2. Selectivity of UV–Vis spectrophotometric method

In order to prevent interferences between CHL and other chemicals contained in microparticle, microneedle, and vaginal tissue during the examination utilizing UV–vis spectrophotometry, a specificity test was conducted [29,33]. As was already noted, the content of CHL in the formulation was determined using the analytical technique in methanol. Additionally, the analytical method's development in PBS, PVA, and TSB was done in order to calculate the CHL *in vitro*, while skin tissue sample was used to calculate the CHL in *ex vivo* studies. Fig. 1 shows representative UV spectra of CHL and several blank in various media.

Based on the analysis results, in all media, the measurement of the blank spectra of MPs, DMN, and skin tissue, there was no peak that appeared at the wavelength of CHL in each medium. These findings showed that the inclusion of additional MPs, DMN, and tissue skin ingredients did not cause any interference [30].

After measurements were made, there was a shift in the optimum absorption, but it was still in the optimum absorption area of CHL in the medium methanol, PBS, and PVA 1%. There was a shift in the absorption of a longer wavelength in TSB media. These results are also consistent with those of Tseplin et al. who found that the particular impact of the polar solvent, which presents itself here as a bathochromic shift of one of the π–π* bands, is generated by the creation of hydrogen bonds between solvent molecules and the molecule as a result, by a decrease in the energy gap between the corresponding occupied (π) and empty (π*) molecular orbitals [35]. Based on the results obtained, the method developed in this study was specific at the appropriate wavelength.

3.3. Linearity, LOD, and LLOQ

In assessing the linearity parameters and determining the rates of LOD and LLOQ from the scientific form, the measurement graph was produced by calculating the CHL standard solution concentration of each medium (methanol, PBS, PVA 1%, and TSB) utilizing the advanced UV–vis spectrophotometry. The spectra of standard solutions across various media are depicted in Fig. 2. Linearity, LOD, and LLOQ settings of the CHL can be seen in Table 4 and Fig. 3.

Based on the data in Table 6, Each calibration curve comprised six concentration levels: 2.5, 5, 10, 20, 30, 40 μg/mL in MeOH, PVA 1%, PBS, and skin tissue media. While the TSB media obtained six concentrations of calibration curves, namely, 125, 250, 500, 750, 1000, and 1250. Since there was no concentration data in the matrix or a similar reference to find out about CHL levels, the concentration points in the calibration curve were used in the calculation.

The slopes and their coefficient of variation as the parameter for analyzing linear equations were determined because they were the most prominent indicator of the sensitivity of analytical methods and their quantification capabilities. Linear relationships were obtained between absorbance and concentration in 2.5–40 μg/mL for CHL-MeOH, CHL-PVA 1%, CHL-PBS, CHL-Skin Tissue and 125–1250 μg/mL for CHL-TSB. The value of the determination coefficient (r^2) of the four CHL regression equations on Methanol, PVA 1%, PBS, skin tissue, and TSB were 0.9981, 0.9993, 0.9975, 0,9981 and 0.9934, respectively. It was shown from the results that the calibration curves determination coefficients (r2) were more than 0.99, and their variation coefficients were less than 25%. Hence, it can be concluded that we satisfied the acceptance criteria, and a high sensitivity was achieved in the four-study media. Therefore, a range of 2.5–40 μg/mL values for CHL-MeOH, CHL-PVA 1%, CHL-PBS, and 125–1250 μg/mL for CHL-TSB can be used for LOD and LLOQ calculations. Quality LOD and LLOQ of CHL inside the methanol were 2.37 and 7.20 μg/mL, on PVA 1% were 1.45 and 4.40 μg/mL, on PBS 2.70 and 8.18, on skin tissue 2.40 and 7.27, and on TSB medium were 127.87 and

Table 7
The Results of evaluation of precision and accuracy of CHL analysis in PBS (mean ± SD, n = 3).

Interday Precision and Accuracy				
Replication	**Concentration added (μg/mL)**	**Found concentration (μg/mL) ± SD**	**Precision (%RSD)**	**Accuracy (%RE)**
1	8.27	8.62 ± 1.17	13.61	−4.23
	12.5	14.02 ± 0.06	0.43	−12.21
	30	31.43 ± 0.13	0.42	4.78
	20	21.96 ± 0.14	0.66	−9.8
2	8.27	8.05 ± 0.15	1.91	2.66
	12.5	13.86 ± 0.36	2.60	−10.88
	30	30.51 ± 0.74	2.42	1.71
	20	21.65 ± 0.60	2.77	−8.25
3	8.27	7.98 ± 0.16	2.09	3.50
	12.5	13.77 ± 0.45	3.28	−10.18
	30	30.93 ± 0.73	2.38	3.11
	20	21.66 ± 0.82	3.81	−8.31
Intraday Precision and Accuracy				
Day	**Concentration added (μg/mL)**	**Found concentration (μg/mL) ± SD**	**Precision (%RSD)**	**Accuracy (%RE)**
1	8.27	7.82 ± 0.15	1.92	5.36
	12.5	13.48 ± 0.34	2.58	−7.84
	30	30.85 ± 0.67	2.18	2.83
	20	21.38 ± 0.12	0.58	−6.91
2	8.27	8.19 ± 0.08	1.08	0.96
	12.5	13.61 ± 0.11	0.81	−8.93
	30	31.2 ± 0.12	0.38	4
	20	21.39 ± 0.06	0.31	−6.98
3	8.27	8.06 ± 0.17	2.12	2.49
	12.5	13.57 ± 0.26	1.95	−8.61
	30	31.27 ± 0.12	0.38	4.23
	20	20.87 ± 0.40	1.94	−4.38

Table 8
The Results of evaluation of precision and accuracy of CHL analysis in TSB (mean ± SD, n = 3).

Interday Precision and Accuracy				
Replication	**Concentration added (μg/mL)**	**Found concentration (μg/mL) ± SD**	**Precision (%RSD)**	**Accuracy (%RE)**
1	388	397.66 ± 15.06	3.78	−2.49
	450	457.66 ± 10.10	2.20	−1.70
	938	922.66 ± 20.81	2.25	−1.63
	600	608.5 ± 16.39	2.69	−1.41
2	388	366 ± 13.91	3.80	5.67
	450	416.83 ± 15.06	3.61	7.37
	938	912.66 ± 5.77	0.63	−2.70
	600	579.33 ± 7.21	1.24	3.44
3	388	369.33 ± 8.77	2.37	4.81
	450	421 ± 9.01	2.14	6.44
	938	894.33 ± 19.41	2.17	−4.65
	600	572.66 ± 10.10	1.76	4.55
Intraday Precision and Accuracy				
Day	**Concentration added (μg/mL)**	**Found concentration (μg/mL) ± SD**	**Precision (%RSD)**	**Accuracy (%RE)**
1	388	363.08 ± 10.77	2.96	6.42
	450	426.83 ± 14.21	3.33	5.14
	938	861.83 ± 18.76	2.17	−8.12
	600	580.16 ± 15.27	2.63	3.30
2	388	340.16 ± 11.54	3.39	12.32
	450	397.66 ± 11.54	2.90	11.62
	938	841 ± 17.32	2.05	−10.34
	600	555.16 ± 14.43	2.59	7.47
3	388	346 ± 10.89	3.14	10.82
	450	401 ± 10	2.49	10.88
	938	850.16 ± 28.75	3.38	−9.36
	600	557.66 ± 17.01	3.05	7.05

387.48 μg/mL.

3.4. Accuracy and precision

Determination of accuracy in intra-day and inter-day amounts using the advanced method exhibited accurate values for PVA 1% (Table 5), methanol (Table 6), PBS (Table 7), TSB (Table 8), skin tissue (Table 9). The measurement of ratio error values is under 15%, which complied the preconditions of the ICH guidelines. Intra-day and inter-day precision were also examined to be adequate. Intra-day and inter-day precision for all solvents determined %RSD values ranging from 0.23% − 13.61% and 0.3% − 3.38% which obeyed the limits of the ICH guidelines (15%) [36]. Thus, the method developed using UV–vis spectrophotometry to determine CHL was found to be accurate and precise.

3.5. Extraction recovery

The quantities of lower limit of quantification (LLOQ), low quality control (LQC), medium quality control (MQC), and high quality control (HQC) extracted from skin tissue were compared to the concentrations obtained by testing samples at the same concentrations to determine the extraction recovery from the technique utilized in this investigation. Table 10 shows the outcomes of the typical extraction recovery. The FDA bioanalytical guideline recommendations emphasize the importance of accuracy, consistency, and reproducibility of recovery, acknowledging that the analyte recovery in bioanalytical methods does not need to be 100%. Additionally, %RSD of the mean extraction recoveries throughout all QC levels was ≤ 15%, indicating the good accuracy, consistency, and reproducibility of the extraction process. As a result, this approach is reliable to measure CHL in rat skin tissue media.

3.6. Application of the analytical method

3.6.1. The properties of analysis and In- vitro release studies of microparticle sensitive bacteria

A UV–vis spectrophotometric method form that has been thoroughly validated was then applied to confirm the quantity of CHL in the microparticle system. The characteristics of the microparticles can be seen in Table 11, and the MPs release profile can be seen in Fig. 5.

The results showed that an analysis from CHL-carried MPs detected by SEM will be visualized in Fig. 4. As shown in SEM images, all formulations were approximately spherical. Notably, the sizes discovered in this study were closely correlated with the findings from SEM analysis and were found to be 0.59 ± 0.02 μm and 1.29 ± 0.09 μm for F1 and F2, respectively. It was found that the particle size of F1 were significantly smaller ($p < 0.05$) compared to F2. It has been postulated that increase in the amount of polymer will increase the particle size due to a rise in the polymer's viscosity, which causes the creation of bigger emulsion droplets and subsequently larger sizes of the microparticle [3738]. For PDI values, it was found that the values were in the range of 0.117 ± 0.01 and 0.121 ± 0.01, demonstrating the generally homogeneous and monodispersed profile of these MPs [39].

Regarding the EE, it was found that the EE of MPs F1 were not significantly different ($p > 0.05$) compared to MPs F2. These results propose that there can be a relatively high amount of CHL that might be entrapped in the PCL MPs. The lower EE may be due to the higher hydrophobicity nature of PCL than CHL. Percentage EE will depend a lot on the polymer type and polymer drug affinity [40]. Therefore, the encapsulation of CHL were low in this polymer. The percentage of encapsulation efficiency in F1 and F2 were 40.94 ± 2.88% and 39.61 ± 3.23, respectively. In terms of DL, the values F1 and F2 were 20.47 ± 1.44 and 13.20 ± 1.07, respectively. Based on the results obtained, the

Table 9
The Results of evaluation of precision and accuracy of CHL analysis in skin tissue (mean ± SD, n = 3).

Interday Precision and Accuracy

Replication	Concentration added (μg/mL)	Found concentration (μg/mL) ± SD	Precision (%RSD)	Accuracy (%RE)
1	7.28	7.61 ± 0.24	3.18	4.47
	10	9.93 ± 0.71	7.11	−0.70
	20	19.42 ± 0,91	4.66	−2.91
	30	31.21 ± 0.67	2.14	4.05
2	7.28	7.80 ± 0.35	4.48	7.08
	10	9.74 ± 0.17	1.71	−2.55
	20	19.64 ± 0.48	2.47	−1.81
	30	32.37 ± 0.46	1.43	7.91
3	7.28	7.84 ± 0.39	4.98	7.69
	10	10.47 ± 0.46	4.41	4.69
	20	20.08 ± 0.51	2.52	0.39
	30	32.08 ± 0.71	2.23	6.93

Intraday Precision and Accuracy

Day	Concentration added (μg/mL)	Found concentration (μg/mL) ± SD	Precision (%RSD)	Accuracy (%RE)
1	7.28	7.43 ± 0.24	3.20	2.00
	10	9.52 ± 0.16	1.71	−4.77
	20	19.22 ± 0.47	2.47	−3.89
	30	31.42 ± 0.70	2.23	4.73
2	7.28	7.66 ± 0.38	5.00	5.15
	10	9.18 ± 0.66	7.19	−8.22
	20	18.66 ± 0.47	2.53	−6.70
	30	30.57 ± 0.65	2.14	1.91
3	7.28	7,61 ± 0.34	4.49	4.56
	10	9,68 ± 0.43	4.45	−3.19
	20	19,01 ± 0.89	4.67	−4.97
	30	31,71 ± 0.45	1.43	5.69

Table 10
Mean extraction recovery of CHL in skin tissue (n = 3).

Sample	Concentration (μg/mL)	%Extraction Recovery ± SD	%RSD
Skin Tissue	LLOQ (5,13)	91.47 ± 1.40	1.53
	QC (7,5)	90.93 ± 1.42	1.56
	MQC (15)	90.84 ± 1.29	1.42
	HQC (24)	91.72 ± 1.73	1.88

Table 11
Results of Measurement of Particle Size, PDI, %EE, and %DL MPs CHL (mean ± SD, n = 3).

Formulation	Particle Size	PDI	% EE	% DL
F1	0.59 ± 0.02	0.117 ± 0.01	40.94 ± 2.88	20.47 ± 1.44
F2	1.29 ± 0.09	0.121 ± 0.01	39.61 ± 3.23	13.20 ± 1.07

increase in the number of polymers (2: 1) in formula 2 decreased the percentage of DL values. This occurred due to the increase of MPs (PCL polymer) composition while retaining the quantity of CHL in the MPs, resulting in a decreasing DL value.

Validated analytical methods also determined the cumulative amount of CHL after *in vitro* release studies on various media. Fig. 5. (A) shows PBS media's *in vitro* release profile. The results showed that the % CHL measured after 24 h in F1 and F2 were 12.75 ± 1.46 and 9.46 ± 1.13, respectively. Fig. 5. (B) shows the MPs release profile *in-vitro* on TSB media. The results showed that the % CHL measured after 24 h in F1 and F2 were 13.41 ± 1.55 and 10.02 ± 1.27, respectively. In both media, it was found that the lower levels of CHL were measured in F1 and F2 when compared to pure CHL due to the absence of a bacterial enzyme stimulus that lyses the PCL polymer so that the drug remains stable in the MPs polymer matrix [41]. The statistical analysis results showed that the release profiles of F1, F2, and CHL, compared to both PBS and TSB media, were not significantly different ($p > 0.05$). This indicated that the media without bacteria did not affect drug release in the bacterial responsive MPs system. Fig. 5. (C) shows *in vitro* release profile of MPs on TSB media and bacteria. The results showed that the % CHL measured after 24 h in F1 and F2 were 99.29 ± 11.10 % and 79.45 ± 9.34 % respectively. In TSB, media containing bacteria showed high drug release. This was due to the SA bacteria culture that produced lipase enzymes that played a role in lysing the MPs matrix to measure CHL levels in the media [17,37].

The statistical analysis results showed significantly different release profile results between bacterial TSB media with PBS and TSB without bacteria. Fig. 5 shows the release profile of pure CHL in all test media showed a rapid drug release profile with levels reaching almost 100% at 3 h, while the microparticle release profile in media containing bacterial stimuli almost reached 100% at 24 h. Fig. 5 shows that the drug release profile of F1 is higher than F2. It is shown that drug release is affected by particle size when drug loading is high (40%). Chen et al also found the same results as we observed regarding the difference in particle size affecting the time and % drug release [42]. The larger surface area of smaller MPs results in a higher concentration of drug molecules at the surface of microspheres, thereby accelerating drug release.

Thus, in contrast to sterile media, the higher release of CHL from PCL MPs in the bacterial system was possible to be an indicator that the bacteria are releasing the enzymes. Additionally, this result was consistent with that of Wu et al., who observed that the addition of an enzyme multiplies PCL degradation by a factor of 1000 compared to degradation in an aqueous medium alone. [43]. A stark contrast between the release of CHL when the bacteria is present or absent demonstrated that the proposed method has the potential for selective delivery at infection sites. Therefore, it was proven from these results that loading CHL into a responsive MPs system can avoid release at non-specific sites.

3.6.2. The properties of analysis and Ex- vivo dermetokinetic studies of microneedle loaded MPs CHL-PCL

For improved penetration profile, the MPs were incorporated into DMN (Fig. 6A and 6B). The quantity of CHL in the microneedle loaded MPs CHL-PCL was also determined using the approved UV–vis spectrophotometry technique. Fig. 6C shows the results, which revealed that 97.64 ± 3.21, 98.09 ± 2.43, and 97.12 ± 2.76 percent of the CHL were recovered from the F1, F2, and Pure CHL in DMN, respectively. These results demonstrated that the concentration of CHL was unaffected by the incorporation of CHL into DMN preparation. All formulations had acceptable recovery percentages, which fell between 95 and 105 percent in accordance with the ICH standard for acceptable recovery percentage [36].

The release kinetics of CHL from MPs after DMN treatments were then examined in a dermatokinetic investigation. The *ex vivo* infection model in rat skins and uninfected skin were used in this investigation. Only choramphenicol released by MPs were measured in order to demonstrate that the presence of bacterial infection had no other effect on the release of CHL in the skin. The skin samples were vortexed with water at each interval to achieve this, to see how much CHL was retained in the skin. Our findings showed that this approach would only extract CHL released from MPs since no CHL was found in the supernatant of MP dispersion.

In this study, we compared the dermatokinetic characteristics of our method to DMNs F1 and F2 with CHL but no MP formulation (DMN-CHL). Fig. 7 shows the concentration of CHL released from MPs in the skin vs application time for the kinetic profiles of CHL in normal skin and *ex vivo* infection models following application of DMNs. Table 12 shows the lists of dermatokinetic profiles of CHL following application of DMNs, including Cmax, Tmax, T1/2, AUC, and MRT. As shown, DMNs-MPs released CHL much less ($p < 0.05$) than DMN- CHL in the absence of

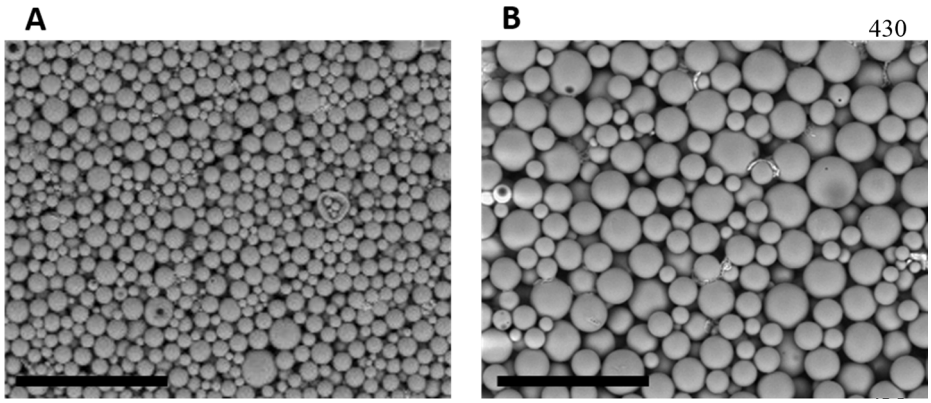

Fig. 4. SEM Visualization Image of F1 (A) and F2 (B) (The black scale bar represents a length of 10 μm in each case).

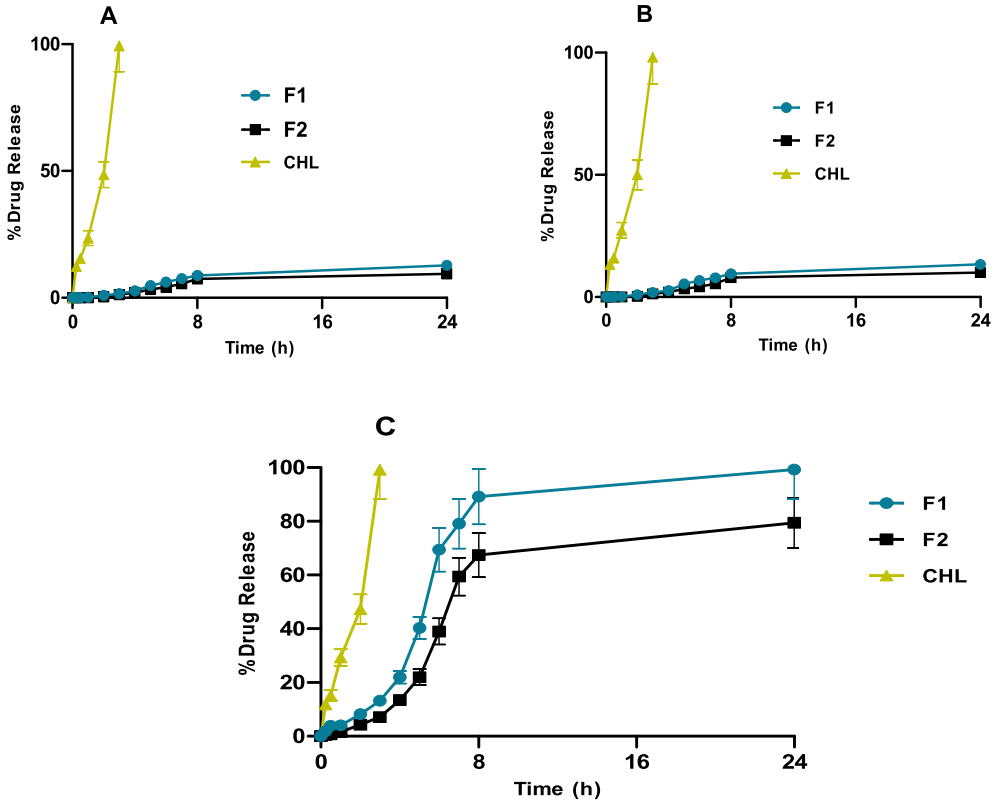

Fig. 5. (A) *in vitro* MPs-CHL release in PBS media, (B) *in vitro* MPs-CHL release in TSB media, (C) *in vitro* MPs-CHL release in TSB + Bacteria media (mean ± SD, n = 3).

bacterial growth in normal skin. The Tmax values of CHL from MN-MPs F1 and F2 were found to be considerably lower ($p < 0.05$) compared to the other formulation due to the explanations provided for the Cmax results. This suggested that the inclusion of CHL into MPs would make it possible to avoid the non-specific release of CHL. The release of CHL from DMN-MPs, in contrast to DMN- CHL, was considerably increased ($p < 0.05$) in *ex vivo* infection models made from SA. The results obtained here indicate that CHL encapsulation in PCL MPs may result in an increase in CHL release via two different processes. The PCL outer layer initially aided in the MPs attachment to the colony infection. Following this, the bacterial strains lipase released into the environment dissolved PCL layers, releasing CHL from MPs. Regarding the impact of pH on kinetical release of CHL in MPs-coated PCL, previous research has demonstrated the profile of nanoparticle release utilizing PCL polymers. The release of carvacrol (CAR) in pure form and CAR-PCL nanoparticles (NPs) was studied at different pH levels in the absence and presence of bacterial lipase enzyme. The result shows that the presence of lipase enzyme has a significantly greater impact on the kinetics of polymer breakdown than the different pH levels ($p < 0.05$) [44]. This explains that the effect of pH resulting from bacterial growth factor does not have a significant impact on the kinetics of CHL release from MPs. Specifically, when compared to the DMN-F2 formula, DMN-F1 had a higher drug release due to the smaller particle size in F1 compared to the F2 formula. In the case of smaller MPs, the greater surface area produces a higher number of drug molecules at the surface of microspheres, thereby accelerating drug release.

Regarding the AUC value, the AUC values of CHL from DMN-MPs specifically F1 in *ex vivo* infection models was discovered to be considerably higher compared to other formulations, demonstrating a good *ex vivo* skin bioavailability of our technique. It was discovered that the

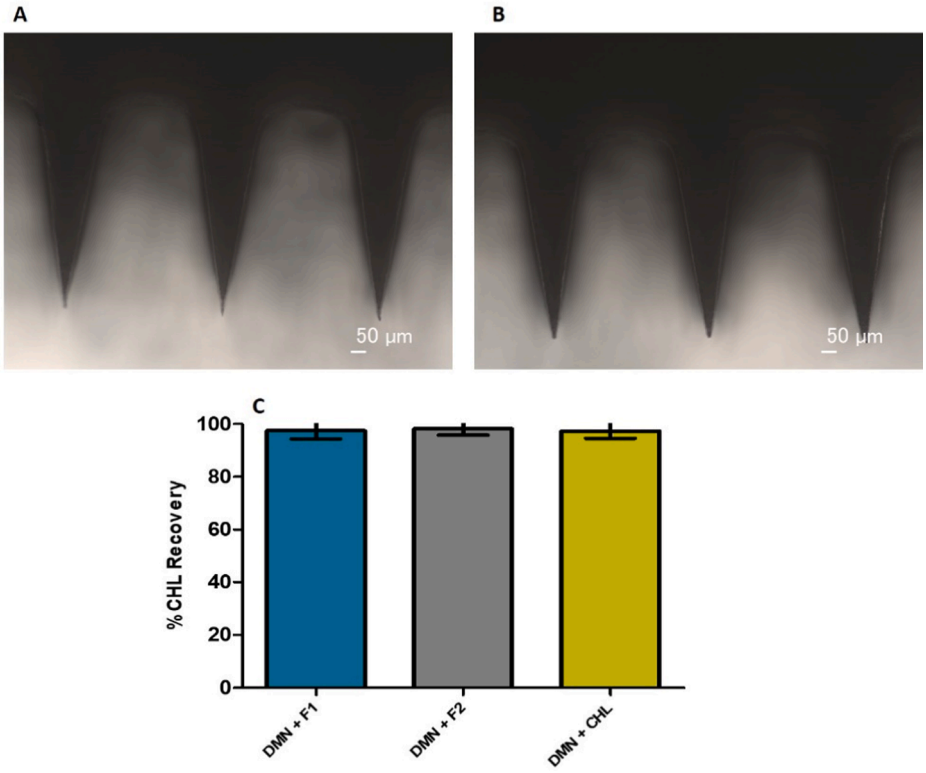

Fig. 6. The microscope images of DMNs containing F1 (A) and F2 (B). CHL recovery (%) from DMN F1, F2, and CHL (C).

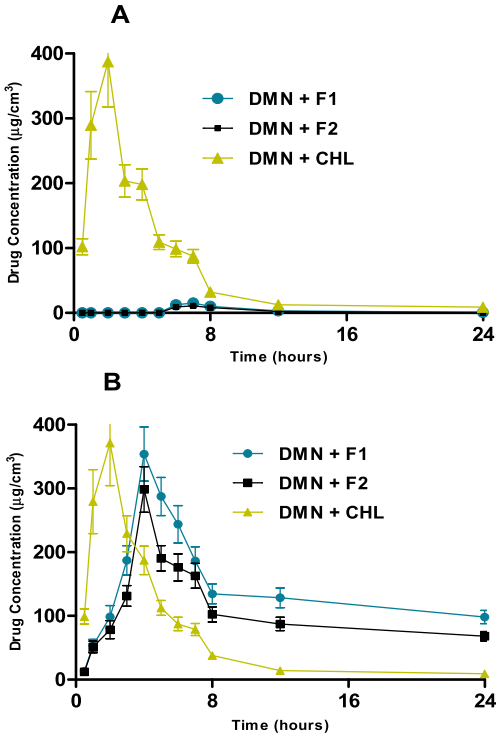

Fig. 7. The *ex vivo* concentrations and time profiles of CHL following the application of DMN-F1, DMN-F2, and DMN-CHL in non-infected rat skin (a), as well as *ex vivo* infection models formed by SA (b).

DMN containing free CHL showed MRT<6 h in terms of retention duration in the infected skin. The MRT values of CHL from DMN-MPs were found to be considerably higher ($p < 0.05$) than those of DMN-CHL, in the case of the retention period in the skin. A lower application time for CHL in the treatment of skin infections may be possible because to the increased MRT. As a result, it can lead to patients accepting this strategy. The combination of responsive MPs and DMNs might successfully transfer chlramphenicol into an *ex vivo* biofilm model, according to our findings.

4. Conclusion

This research aimed to maturate and confirm a CHL analysis procedure that utilizes a UV–vis spectrophotometric method. This study's proposed method went through a validation process with these five parameters: accuracy, precision, linearity, LOD, LLOQ, and extraction recovery. The outcomes indicated which total recognition specifications were right defined and satisfied all of the qualifications from the ICH instructions. In addition, an accepted scientific method was successfully used to calculate the characteristics of the entrapment efficiency, drug loading, percentage recovery, drug release profile of MPs CHL-PCL, and *ex vivo* dermatokinetic of microneedle MPs CHL-PCL. To conclude, the method that has been validated has numerous applications for CHL studies to formulate and characterize bacterial responsive microparticle and microneedle systems.

CRediT authorship contribution statement

Mukarram Mudjahid: Conceptualization, Data curation, Investigation, Methodology, Project administration, Validation, Writing – original draft, Writing – review & editing. **Sulistiawati:** Methodology, Software, Validation, Visualization, Writing – review & editing. **Rangga Meidianto Asri:** Validation, Writing – review & editing. **Firzan Nainu:** Validation, Supervision. **Andi Dian Permana:** Conceptualization, Funding acquisition, Project administration, Supervision, Writing – review & editing.

Table 12
Lists the dermatokinetic characteristics of CHL in uninfected rat skin as well as ex infection models created by SA after the administration of DDMN-F1, DMN-F2, and DMN-CHL. (means SD, n = 3).

Parameter	Unit	DMN + F1		DMN + F2		DMN + CHL	
		Normal	Infection	Normal	Infection	Normal	Infecion
t1/2	h	4.35 ± 0.47	34.20 ± 3.76	3.28 ± 0.36	28.50	4.04 ± 0.44	4.14 ± 0.45
Tmax	h	7 ± 0.91	4 ± 0.52	7 ± 0.91	4 ± 0.52	2 ± 0.26	2 ± 0.26
Cmax	$\mu g/cm^3$	15.02 ± 1.86	353.98 ± 43.89	10.87 ± 1.34	298.34 ± 36.99	387.35 ± 48.03	371.23 ± 46.03
AUC 0-t	$\mu g/cm^3.h$	111.65 ± 13.50	3355.96 ± 406,07	79.20 ± 9.53	2444.10 ± 295.73	1583.74 ± 191.63	1587.71 ± 192.11
AUC 0-inf_obs	$\mu g/cm^3.h$	117.12 ± 15.46	8203.39 ± 1082.84	80.52 ± 10.62	5246.17 ± 692.49	1634.65 ± 215.77	1642.79 ± 216.84
MRT 0-inf_obs	h	9.80 ± 1.16	47.67 ± 5.67	8.59 ± 1.02	39.58 ± 4.71	5.36 ± 0.63	5.56 ± 0.66

Declaration of Competing Interest

The authors declare that they have no known competing financial interests or personal relationships that could have appeared to influence the work reported in this paper.

Data availability

Data will be made available on request.

Acknowledgement

Mukarram Mudjahid is thankful for the scholarship provided by German Academic Exchange Service (DAAD) (Ref. no. 91818036). This study was also supported by Penelitian Tesis magister, Ministry of Education, Culture, Research, and Technology of Republic of Indoenasia (090/E5/PG.02.00/PT/2022).

References

[1] A.B. Raff, D. Kroshinsky, Cellulitis A Review, Jama 316 (3) (2016) 325–337, https://doi.org/10.1001/jama.2016.8825.
[2] R. Rrapi, S. Chand, D. Kroshinsky, Cellulitis: A review of pathogenesis, diagnosis, and management, Med. Clin. North Am. 105 (4) (2021) 723–735, https://doi.org/10.1016/j.mcna.2021.04.009.
[3] S.M. Ellis Simonsen, et al., Cellulitis incidence in a defined population, Epidemiol. Infect. 134 (2) (2006) 293–299, https://doi.org/10.1017/S095026880500484X.
[4] C.A. Andersen, K. McLeod, R. Steffan, Diagnosis and treatment of the invasive extension of bacteria (cellulitis) from chronic wounds utilising point-of-care fluorescence imaging, Int. Wound J. no. September (2021) 1–13, https://doi.org/10.1111/iwj.13696.
[5] E.L.A. Cross, et al., Route and duration of antibiotic therapy in acute cellulitis: A systematic review and meta-analysis of the effectiveness and harms of antibiotic treatment, J. Infect. 81 (4) (2020) 521–531, https://doi.org/10.1016/j.jinf.2020.07.030.
[6] O. Uddin, J. Hurst, T. Alkayali, S.A. Schmalzle, Staphylococcus hominis cellulitis and bacteremia associated with surgical clips, IDCases 27 (2022) e01436.
[7] J.L.P. Gemeinder, et al., Gentamicin encapsulated within a biopolymer for the treatment of Staphylococcus aureus and Escherichia coli infected skin ulcers, J. Biomater. Sci. Polym. Ed. 32 (1) (2021) 93–111, https://doi.org/10.1080/09205063.2020.1817667.
[8] S. Sartini, et al., Current state and promising opportunities on pharmaceutical approaches in the treatment of polymicrobial diseases, Pathogens 10 (2) (2021) 1–31, https://doi.org/10.3390/pathogens10020245.
[9] S. Kalita, et al., Chloramphenicol encapsulated in poly-ε-caprolactone-pluronic composite: Nanoparticles for treatment of MRSA-infected burn wounds, Int. J. Nanomedicine 10 (2015) 2971–2984, https://doi.org/10.2147/IJN.S75023.
[10] M. Abdollahi, S. Mostafalou, Chloramphenicol, Encycl. Toxicol. Third Ed. 1 (2014) 837–840, https://doi.org/10.1016/B978-0-12-386454-3.00709-0.
[11] P. Shukla, F.W. Bansode, R.K. Singh, Chloramphenicol Toxicity : A Review, J. Med. Med. Sci. 2 (13) (2011) 1313–1316.
[12] I.S. Ferreira, et al., Activity of daptomycin- and vancomycin-loaded poly-epsilon-caprolactone microparticles against mature staphylococcal biofilms, Int. J. Nanomedicine 10 (2015) 4351–4366, https://doi.org/10.2147/IJN.S84108.
[13] T.W. Prow, et al., Nanoparticles and microparticles for skin drug delivery, Adv. Drug Deliv. Rev. 63 (6) (2011) 470–491, https://doi.org/10.1016/j.addr.2011.01.012.
[14] A.D. Permana et al., Selective delivery of silver nanoparticles for improved treatment of biofilm skin infection using bacteria-responsive microparticles loaded into dissolving microneedles, Mater. Sci. Eng. C, vol. 120, no. November 2020, p. 111786, 2021, doi: https://doi.org/10.1016/j.msec.2020.111786.
[15] N. Devnarain, et al., Intrinsic stimuli-responsive nanocarriers for smart drug delivery of antibacterial agents—An in-depth review of the last two decades, Wiley Interdiscip. Rev. Nanomedicine Nanobiotechnology 13 (1) (2021) 1–38, https://doi.org/10.1002/wnan.1664.
[16] L. Van Gheluwe, I. Chourpa, C. Gaigne, E. Munnier, Polymer-based smart drug delivery systems for skin application and demonstration of stimuli-responsiveness, Polymers (Basel)., vol. 13, no. 8, 2021, doi: https://doi.org/10.3390/polym13081285.
[17] H. Chen, et al., Design of smart targeted and responsive drug delivery systems with enhanced antibacterial properties, Nanoscale 10 (45) (2018) 20946–20962, https://doi.org/10.1039/c8nr07146b.
[18] Y. Li, G. Liu, X. Wang, J. Hu, S. Liu, Enzyme-responsive polymeric vesicles for bacterial-strain-selective delivery of antimicrobial agents, Angew. Chemie - Int. Ed. 55 (5) (2016) 1760–1764, https://doi.org/10.1002/anie.201509401.
[19] M.H. Xiong, Y. Bao, X.Z. Yang, Y.C. Wang, B. Sun, J. Wang, Lipase-sensitive polymeric triple-layered nanogel for 'on-demand' drug delivery, J. Am. Chem. Soc. 134 (9) (2012) 4355–4362, https://doi.org/10.1021/ja211279u.
[20] A.D. Permana, M.T.C. McCrudden, R.F. Donnelly, Enhanced intradermal delivery of nanosuspensions of antifilariasis drugs using dissolving microneedles: A proof of concept study, Pharmaceutics 11 (7) (2019) 1–22, https://doi.org/10.3390/pharmaceutics11070346.
[21] A.J. Paredes, et al., Microarray Patches: Poking a Hole in the Challenges Faced When Delivering Poorly Soluble Drugs, Adv. Funct. Mater. 31 (1) (2021) 1–27, https://doi.org/10.1002/adfm.202005792.
[22] D. Karunakaran, et al., Design and Testing of a Cabotegravir Implant for HIV Prevention, J. Control. Release 330 (2021) 658–668.
[23] F.P. Pons-Faudoa, et al., 2-Hydroxypropyl-β-cyclodextrin-enhanced pharmacokinetics of cabotegravir from a nanofluidic implant for HIV pre-exposure prophylaxis, J. Control. Release 306 (2019) 89–96.
[24] Sulistiawati, et al., Validation of spectrophotometric method to quantify cabotegravir in simulated vaginal fluid and porcine vaginal tissue in ex vivo permeation and retention studies from thermosensitive and mucoadhesive gels, Spectrochim. Acta - Part A Mol. Biomol. Spectrosc. 267 (2022), 120600, https://doi.org/10.1016/j.saa.2021.120600.
[25] S. Gorantla, R.N. Saha, G. Singhvi, Spectrophotometric method to quantify tofacitinib in lyotropic liquid crystalline nanoparticles and skin layers: Application in ex vivo dermal distribution studies, Spectrochim. Acta - Part A Mol. Biomol. Spectrosc. 255 (2021), 119719.
[26] A. Mahmood, et al., UV spectrophotometric method for simultaneous estimation of betamethasone valerate and tazarotene with absorption factor method: Application for in-vitro and ex-vivo characterization of lipidic nanocarriers for topical delivery, Spectrochim. Acta - Part A Mol. Biomol. Spectrosc. 235 (2020), 118310.
[27] H.E. Putri et al., Dissolving Microneedle Formulation of Ceftriaxone: Effect of Polymer Concentrations on Characterisation and Ex Vivo Permeation Study, J. Pharm. Innov., no. 0123456789, 2021, doi: https://doi.org/10.1007/s12247-021-09593-y.
[28] D. Ramadon, et al., A sensitive HPLC-UV method for quantifying vancomycin in biological matrices: Application to pharmacokinetic and biodistribution studies in rat plasma, skin and lymph nodes, J. Pharm. Biomed. Anal. 189 (2020), 113429.
[29] A.D. Permana, et al., New and sensitive HPLC-UV method for concomitant quantification of a combination of antifilariasis drugs in rat plasma and organs after simultaneous oral administration, Anal. Methods 13 (7) (2021) 933–945.
[30] J.T. do P. Silva et al., Analytical validation of an ultraviolet–visible procedure for determining lutein concentration and application to lutein-loaded nanoparticles, Food Chem., vol. 230, pp. 336–342, 2017, doi: https://doi.org/10.1016/j.foodchem.2017.03.059.
[31] M.S. Raghu, K. Basavaiah, Two charge-transfer complexation reactions for spectrophotometric determination of pheniramine maleate using π-acceptors, J. Sci. Ind. Res. (India) 70 (10) (2011) 851–858.
[32] N. Alhusein, I.S. Blagbrough, M.L. Beeton, A. Bolhuis, P.A. De Bank, Electrospun Zein/PCL Fibrous Matrices Release Tetracycline in a Controlled Manner, Killing Staphylococcus aureus Both in Biofilms and Ex Vivo on Pig Skin, and are Compatible with Human Skin Cells, Pharm. Res. 33 (1) (2016) 237–246, https://doi.org/10.1007/s11095-015-1782-3.
[33] A.D. Permana, et al., Solid lipid nanoparticle-based dissolving microneedles: A promising intradermal lymph targeting drug delivery system with potential for

enhanced treatment of lymphatic filariasis, J. Control. Release 316 (September) (2019) 34–52, https://doi.org/10.1016/j.jconrel.2019.10.004.
[34] Y. Zhang, M. Huo, J. Zhou, S. Xie, PKSolver: An add-in program for pharmacokinetic and pharmacodynamic data analysis in Microsoft Excel, Comput. Methods Programs Biomed. 99 (3) (2010) 306–314, https://doi.org/10.1016/j.cmpb.2010.01.007.
[35] E.E. Tseplin, S.N. Tseplina, O.G. Khvostenko, Mechanisms of specific effects of polar solvent in optical absorption spectra, Opt. Spectrosc. (English Transl. Opt. i Spektrosk. 110 (6) (2011) 903–909, https://doi.org/10.1134/S0030400X11060166.
[36] ICH, International Conference on Harmonisation, in: Validation of Analytical Procedures: Text and Methodology Q2(R1),1994 (2005).
[37] M. Kiliçarslan, T. Baykara, The effect of the drug/polymer ratio on the properties of the verapamil HCl loaded microspheres, Int. J. Pharm. 252 (1–2) (2003) 99–109, https://doi.org/10.1016/S0378-5173(02)00630-0.
[38] N. Sharma, P. Madan, S. Lin, Effect of process and formulation variables on the preparation of parenteral paclitaxel-loaded biodegradable polymeric nanoparticles: A co-surfactant study, Asian J. Pharm. Sci. 11 (3) (2016) 404–416, https://doi.org/10.1016/j.ajps.2015.09.004.
[39] C. Folle, et al., Thymol-loaded PLGA nanoparticles: an efficient approach for acne treatment, J. Nanobiotechnology 19 (1) (2021) 1–21, https://doi.org/10.1186/s12951-021-01092-z.
[40] M.M. Badran, A.H. Alomrani, G.I. Harisa, A.E. Ashour, A. Kumar, A.E. Yassin, Novel docetaxel chitosan-coated PLGA/PCL nanoparticles with magnified cytotoxicity and bioavailability, Biomed. Pharmacother. 106 (July) (2018) 1461–1468, https://doi.org/10.1016/j.biopha.2018.07.102.
[41] M. Mir, N. Ahmed, A.D. Permana, A.M. Rodgers, R.F. Donnelly, A.U. Rehman, Enhancement in site-specific delivery of carvacrol against methicillin resistant staphylococcus aureus induced skin infections using enzyme responsive nanoparticles: A proof of concept study, Pharmaceutics, vol. 11, no. 11. 2019, doi: https://doi.org/10.3390/pharmaceutics11110606.
[42] W. Chen, A. Palazzo, W.E. Hennink, R.J. Kok, Effect of particle size on drug loading and release kinetics of gefitinib-loaded PLGA microspheres, Mol. Pharm. 14 (2) (2017) 459–467, https://doi.org/10.1021/acs.molpharmaceut.6b00896.
[43] C. Wu, T.F. Jim, Z. Gan, Y. Zhao, S. Wang, "A heterogeneous catalytic kinetics for enzymatic biodegradation of poly (e -caprolactone) nanoparticles in aqueous solution" 41 (2000) 3593–3597.
[44] M. Mir, A.D. Permana, N. Ahmed, G.M. Khan, A. ur Rehman, R.F. Donnelly, Enhancement in site-specific delivery of carvacrol for potential treatment of infected wounds using infection responsive nanoparticles loaded into dissolving microneedles: A proof of concept study, Eur. J. Pharm. Biopharm., vol. 147, no. December 2019, pp. 57–68, 2020, doi: https://doi.org/10.1016/j.ejpb.2019.12.008.